UNIVERSIDAD POLITÉCNICA DE MADRID

ESCUELA TÉCNICA SUPERIOR DE INGENIERÍA AGRONÓMICA, ALIMENTARIA Y DE BIOSISTEMAS

MASTER IN COMPUTATIONAL BIOLOGY

DEPARTAMENTO DE BIOTECNOLOGÍA-BIOLOGÍA VEGETAL – ETSIAAB

DEPARTMENT OF CRYSTALLOGRAPHY AND STRUCTURAL BIOLOGY – INSTITUTO DE QUÍMICA FÍSICA ROCASOLANO, CSIC

Chemical control of the pathway leading to drought tolerance in plants.

TRABAJO FIN DE MÁSTER

Autor: Ángela Gómez Sacristán

Tutor Externo: Armando Albert de la Cruz

Tutor Académico: María Garrido Arandia

July, 2023

Table of Contents:

1. SUMMARY

In recent years, the impact of climate change has intensified water scarcity and irregular rainfall. These circumstances represent two significant challenges for plants, which, in turn, hinder crop productivity and pose a serious threat to the sustainability of agriculture.

At the plant level, major water loss occurs by transpiration when stomata are open, a process which is regulated by intrinsic signals such as the phytohormone Abscisic Acid (ABA). The characterisation of the proteins involved in the ABA pathway has led to a new field of research aimed at the discovery of ABA mimicking molecules. These molecules are capable to regulate exogenously stomata function thus, acting as agrochemical compounds against drought stress. The characterization of Nicotinic Acid as an ABA antagonist has provided a starting point for the discovery of Nicotinic acid related compounds with ABA related bioactivity.

This study employs the high-resolution structural information derived from the proteins involved in the ABA recognition pathway to find environmentally friendly agrochemical compounds that exogenously might control the ABA-dependent response of the pathway. For this purpose, an *in silico* screening of a library of compounds against ABA receptors was performed and the hits derived from this study were validated experimentally.

Docking studies, based on a self-made docking protocol, against a self-made database of natural compounds, gave rise to 4 hits whose experimental validation showed Nicotinamide Ribose (NR) as a possible eco-friendly candidate to control the ABA-dependent response of the pathway. Future *in vitro* assays on the other receptors of the family and *in vivo* assays in plants should be performed to corroborate this.

Keywords: ABA, Nicotinic Acid, drought stress, docking, CsPYL1, HAB1, Nicotinamide Ribose, NR.

2. INTRODUCTION

2.1 Drought as a limitation for crop productivity

Water limitation and irregular rainfall are two of the main adversities for plants. In recent years, both have been aggravated by climate change, threatening the sustainability of agriculture. Thus, the rise in temperatures and the change un rainfall patterns result not only in direct effects on crop yields, but also in indirect effects through changes in the availability of irrigation water [(1)].

In the face of drought stress, plants show responses that tend to avoid it or mechanisms or adaptations to tolerate it. In most plants, both strategies coexist, as in the case of Mediterranean ecosystems where the species that suffer greater drought stress are those that show greater transpiration [(2)].

2.2 Plant transpiration through stomata

Plant transpiration comprises the process of water evaporation through the stomata. Together with carbon dioxide (CO_2) exchange, it determines the water use efficiency (WUE) of a plant. Transpiration also involves the transport of nutrients and water from the roots to the aerial parts of the plant [(3)].

Stoma complexes are found in the epidermis of the aerial parts of plants, such as leaves. Stoma is composed of two guard cells flanking a small pore. These guard cells are able, through turgor changes, to increase and decrease the size of the pore. In this way, both CO_2 influx and transpiration are regulated. Therefore, the role of stomata in the regulation of gas exchange between the plant and the atmosphere is crucial and determines WUE [(4)].

Stomatic closure and opening not only occur in response to environmental signals, such as CO_2 or light, but also to intrinsic signals from the plant itself, such as the hormone ABA [(5)].

2.3 Pythormone ABA

ABA is a plant hormone or phytohormone involved in two of the basic processes for plant development. On the one hand, it intervenes in the regulation of seed maturation and germination: in the processes of dormancy acquisition, accumulation of nutrient reserves and acquisition of tolerance to desiccation. On the other hand, it intervenes in the process of plant adaptation to different types of environmental stress, such as cold, salinity and drought [6]. Stomatal closure is a physiological resistance mechanism against drought stress. This process of stomata closure is largely regulated by ABA [7].

Following the observation of increased ABA levels in vegetative plant tissues to these stresses, it was determined that the plant hormone ABA was one of the mediators of these responses. Thus, ABA levels in the plant are determinants of the behaviour of the plant under stress conditions. These levels are modulated by a precise balance between biosynthesis and catabolism of this phytohormone [8].

The ABA content in the leaf increases not only due to its synthesis and transport from the roots, but also due to the decompartmentalization and redistribution of mesophyll cells from chloroplasts. ABA is eventually released into the apoplast (the peripheral extracellular space through which water and nutrients flow) and finally reaches the guard cells of the stomata through the transpiration stream [9]. ABA produces a loss of K^+ cations, Cl^- anions and malic acid in these guard cells, causing an outflow of water from the cytoplasm and resulting in the closure of the stoma [10].

ABA is perceived by the PYR/PYL/RCAR family of ABA receptors and the clade A subfamily of protein phosphatases type-2C (PP2C). ABA receptors are distributed in three families; whereas subfamilies I and II include monomeric receptors, subfamily III includes dimeric ones [11]. In the resting state, these receptors present two conserved loops that flank an open ABA-binding cavity. Those loops are named *Gate* and *Latch* [12]. The dissociation of dimeric receptors and the activation of the monomeric ones result from ABA-induced conformational rearrangements. Another important conformational rearrangements are those related with *Latch* and *Gate* loops which are required for the surface definition where the receptor would be able to dock to the active site of the PP2C [13]. Protein phosphatases type-2C (PP2C) act as necessary ABA co-receptors as for the

formation of PYR/PYL/RCAR-ABA-PP2C ternary complexes are required to transmit the ABA signals [14]. When ABA concentration increases, PP2C-SnRK2 complexes dissociate due to the formation of those receptor-ABA-phosphatase complexes. This dissociation suppresses the PP2C-mediated SnRK2 inhibition (***Figure 1***). Thus, ABA response is triggered. In addition, in order to reactivate SnRK2s that were dephosphorylated by PP2Cs, some RAF-like MAPKKKs are required [11].

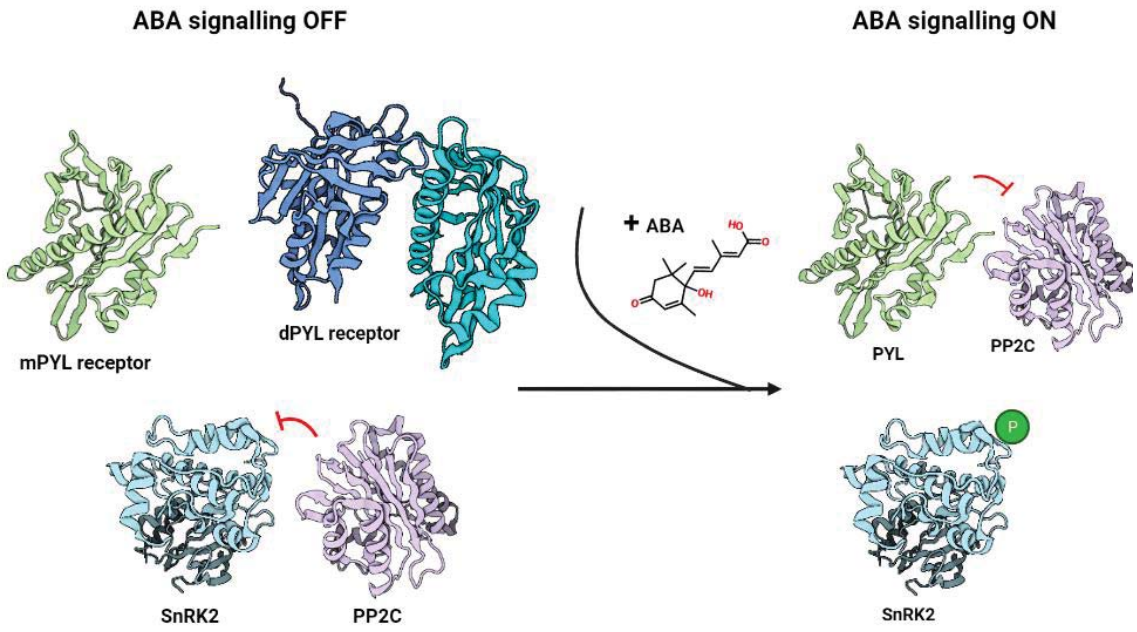

Figure 1. ABA signalling. ABA Receptors compete with SnRK2 for the active site of the PP2C. Receptor-ABA-phosphatase complex formation triggers ABA response. "mPYL" and "dPYL" receptor stands for monomeric and dimeric receptor, respectively.

2.4 Nicotinic acid

Studies on the characterization of the ABA pathway have given way to a new field of research aimed at the design and characterization of new natural compounds capable of acting as agrochemical compounds against stress. In particular, ABA agonist and antagonist molecules capable of exogenously and dynamically modulating the signalling of this phytohormone and, therefore, the responses derived from it [15].

Recently, crystallographic studies on a mutated tomato ABA receptor called SlPYL1

E151D, revealed Nicotinic Acid, also known as niacin or Vitamin B3, as an ABA antagonist molecule. The study showed how the ABA-binding site was blocked by two niacin molecules. The binding of this molecule at the ABA-binding site result in the stabilization of the *Latch* loop in an unproductive conformation that prevents *Gate* loop closure [16]. These studies revealed that niacin is 100 times less potent than other better known ABA antagonists such as opabactin but it is worth mentioning that niacin is a precursor of NAD (nicotinamide adenine dinucleotide), a compound involved in the stress response in plants [17] and present in high concentrations in plant tissues.

Therefore, we reasoned that natural compounds that bind ABA receptors, such as Nicotinic Acid, could be considered interesting lead compounds for the discovery of new agrochemical compounds against drought stress.

2.5 Objectives

In view of all of the above, the main objective of this study is to employ the high-resolution structural information derived from the proteins involved in the ABA recognition pathway to find an environmentally friendly agrochemical compound that exogenously controls the ABA-dependent response of the pathway. For this purpose, an *in silico* screening of a library of natural compounds against ABA receptors will be performed and the hits derived from this study will be validated experimentally.

3. MATERIAL AND METHODS

3.1 Bioinformatic approach

3.1.1 Ligand-Receptor interactions study

Interactions that occurred between the ABA receptors and the ABA and Nicotinic Acid molecules were studied using PyMOL, a molecular visualization system distributed by Schrödinger [18].

3.1.2 *In silico* screening and data curation

To perform the *in silico* screening of potential candidate ligands for binding the ABA receptor Arthor was used. Arthor is a high-performance chemical database searching engine that filters by substructures using the SMILES Arbitrary Target Specification (SMARTS, a chemical notation to represent chemical structures) and by similarity using fingerprint-based Tanimoto scores. Arthor combines more than 25 databases including ZINC database, Mcule and ChemSpace [(19)]. Filters 'Metabolite' and 'Organic Compound' were used during the screening.

Besides, after the creation of a small self-made database with the possible candidate ligands for docking assays (around 500), all the ligands were curated. For this purpose, Coot [(20)], a molecular model building program; and Mercury [(21)], a CCDC program for molecule building, modelling and curation, were used. The curation process for all ligands involved the ionization at the plant physiological pH, hydrogens addition and conformers generation.

In addition, docking assays also required the preparation of the target protein. For this purpose, a template file based on the structure of CsPYL1 ABA receptor (PDB code 5MN0) was prepared in which the following adjustments were made: heteroatoms removal, hydrogens addition and waters edition. The waters edition adjustment consisted of removing all the waters and then including a consensus of structural waters involved in the interactions of the different ligands studied; thus, 6 water molecules were included (coordinates available in ***Table 3***, ***Annex***). In general, the coordinates of the water molecules were chosen by averaging the different coordinates of the conserved and equivalent water molecules found in the experimental structures of different ABA receptors.

3.1.3 Docking studies and protocols

Docking, also known as molecular docking, is the prediction of the binding between proteins and ligands, taking into account the different energies and types of bonds.

Both, the creation of docking protocols and the performance of docking studies, were performed using CCDC's GOLD [(22)] program. The main feature of this program is that it

allows the scores obtained in the docking to be adjusted according to values such as "constraint weight", "fitting point weight" or "score contribution per atom found in region" given to the different regions of the designed pharmacophore. It allows to perform highly accurate dockings focusing on the physico-chemical interactions that occur between the receptor and the different ligands.

Docking studies were performed with all the ligands of the self-made database. After analysing the scores obtained and detecting possible candidate molecules, the latter were validated by generating -*with Mercury* [21]-, and launching for docking -*with GOLD* [22]- around 200 conformers of each one.

3.2 Expression and purification of proteins

3.2.1 Protein expression

The expression of the CsPYL1 receptor was performed in *Escherichia coli* (*E. coli*) cells of *BL21* strain previously transformed with the pETM11 vector containing the gene coding for the CsPYL1 protein labelled with a six His-Tag at C-terminus and the kanamycin resistance gene. From a stock of these transformed cells stored in glycerol, a *starter culture*, i.e. a pre-culture, was prepared. For this, under sterile conditions, 1 µL of the transformed cells stored in glycerol and 10 µL of kanamycin were added to 15 µL of 2TY medium (composed of 16 g/L tryptone, 10 g/L yeast extract and 5 g/L NaCl). It was then incubated with shaking at 220 rpm and 37°C O/N (overnight). After the incubation time, under sterile conditions, 700 ml of 2TY medium were inoculated using the *starter culture* and incubated at 220 rpm (revolutions per minute) and 37ºC until an optical density (O.D.) measured at Absorbance 600 nm of 0.6-0.8 was reached (these A_{600} values correspond to the exponential phase of bacterial growth, i.e. the phase in which metabolism is most optimal). Once these A_{600} values were reached, CsPYL1 protein expression was induced in the culture by adding 300 µL of β-D-1-thiogalactopyranoside (IPTG). Finally, it was incubated at 220 rpm and 16°C O/N. The next day, the IPTG-induced culture was centrifuged at 4750 rpm and 4°C for 20 minutes, obtaining a pellet of the transformed and expressed cells ready for its purification.

3.2.2 Protein purification

Cell pellet was resuspended in 40 mL of lysis buffer (consisting of 25 mM Tris pH 8, 200 mM NaCl, 15 mM imidazole, 5 mM β-mercaptoethanol, 20 µL DNase 10 mg/mL and 50 µL phenylmethylsulfonyl fluoride (PMFS) 0.1 M) and then sonicated for 7 min on ice in cycles of 10" ON followed by 10" OFF. The cell lysates were clarified by centrifugation at 30000 rpm and 4°C for 40 minutes, and then the supernatants, also called soluble fraction, were collected. The purification of CsPYL1 consists of two serial chromatographies: a nickel-histidine affinity chromatography (immobilised metal affinity chromatography, IMAC) and a size-exclusion chromatography (SEC).

Nickel-histidine affinity chromatography

After the cell lysis, the soluble fraction was passed through a 1mL Nickel (Ni^{2+}) column (Cytiva HisTrap™ high performance columns pre-packed with Ni Sepharose™) previously washed with 10 column volumes of H_2O and equilibrated with another 10 column volumes of base buffer (composed of 25 mM Tris pH 8, 200 mM NaCL, 15 mM imidazole and 5 mM β-mercaptoethanol). The column was then washed with 10 column volumes of base buffer followed by 10 column volumes of a buffer composed of base buffer and 40 mM imidazole. Finally, the protein was eluted by addition of elution buffer (composed of base buffer and 500 mM imidazole); 1 mL fractions were collected from this elution.

Nanodrop-measured 1 mg/mL absorbance and the molar extinction coefficient of CsPYL1 were used to determine the concentration of the protein contained in each of the 1 mL fractions collected. Fractions containing a concentration greater than 0.29 mg/mL protein and an optimal A260/A280 ratio (between approximately 0.5-0.8) were pooled.

The fraction obtained from the pooling of these fractions was subjected to a dialysis process. TEV protease (a protease capable of cleaving His-Tag) was added to this fraction. In addition, it itself also possesses one, although it is not able to cleave itself) at a ratio of 1:40 compared to the eluted protein. The mixture of protein and TEV was placed on a dialysis membrane and left to cleave O/N at 4°C in front of a dialysis buffer composed of 25 mM Trish pH 8 and 5 mM β-mercaptoethanol in order to remove salts.

Thus, after dialysis, the cleaved protein and TEV would be obtained inside the membrane.

The next day, the Nickel column was again equilibrated with a buffer of the same composition as the dialysis buffer and the contents of the membrane (i.e. the cleaved protein and the TEV) were passed through it. Thus, as the TEV was retained (due to its own His-Tag), the resulting elution from the column would be only the cleaved protein. This elution was therefore collected.

Size-exclusion chromatography (SEC)

The previously collected eluted cleaved protein was subjected to size-exclusion chromatography. The first step was to wash the size-exclusion chromatography column to be used (Superdex 200 HiLoad 16/60 TM) with H_2O for 24 hours. Then, the column was equilibrated with a buffer composed of 25 mM Tris pH 8 and 5 mM β-mercaptoethanol. Finally, the protein was passed through the column at a flow rate of 1 ml/min and 1 ml fractions were collected, pooled and concentrated.

To check the purity of the protein and the quality of the purification process, SDS-PAGE gel electrophoresis of the 12% acrylamide.

3.3 Affinity studies

3.3.1 HAB1 phosphatase activity assay

The following samples were prepared: HAB1 at 0.25 µM, HAB1-CsPYL1 in a 1:4 ratio (0.25 µM : 1 µM), HAB1-CsPYL1-ABA (ABA at 250 nM), HAB1-CsPYL1-R (R -*Ribosylnicotinate*- at 100 µM), HAB1-CsPYL1-NR (NR -*Nicotinamide Ribose*- at 100 µM), HAB1-CsPYL1-Nmn (Nmn -*Nicotinamide mononucleotide*- at 100 µM) and HAB1-CsPYL1-β-R (β-R -*Nicotinate Beta-D-Ribonucleotide*- at 100 µM). Note: in the ligand-bound samples, HAB1 and CsPYL1 were always in a 1:4 ratio (0.25 µM HAB1 : 1 µM CsPYL1).

Thus, the different samples were prepared adjusting to a final reaction volume of 100 µL which contained, in addition to the mentioned ratios of HAB1 phosphatase, CsPYL1 receptor and ligand; DTT (dithiothreitol) and $MnCl_2$ at 1 mM concentration and pNPP at

25 mM.
It should be noted that, due to its high photosensitivity, pNPP was the last element added to the final reaction volume.
For each sample, 4 replicates were performed. These replicates were placed in a 96-well plate and their absorbances at 405 nm were measured at 0 minutes and 15 minutes. The absorbances were measured on the Bio-Rad ™ 3550 Microplate Reader.

The percentage phosphatase activity of each sample was calculated as follows. For each replicate, the Abs_{405} nm value at time 15 minus the Abs_{405} nm value at time 0 min was subtracted. Then, the replicates of the different samples were averaged by eliminating the outliers. After averaging, the average value of the HAB1-CsPYL1 sample was assigned as 100% of the phosphatase activity, as this sample, in the background, represents the basal inhibition of HAB1 phosphatase. Finally, the percentage of phosphatase activity of the remaining samples was calculated by a rule of three with 100%. Once the results were obtained, a Student's t-test was performed between the different samples with the HAB1 sample (control). This statistical analysis was performed in GraphPad Prism 9.0 software.

3.3.2 IC_{50} determination

The determination of the IC_{50} of NR was also carried out by means of a phosphatase activity assay with pNPP. In this case, the samples prepared were: HAB1-CsPYL1 in a 1:4 ratio (0.25 µM : 1 µM), HAB1-CsPYL1-NR (NR -*Nicotinamide Ribose*- at 20 mM), HAB1-CsPYL1-NR (NR -*Nicotinamide Ribose*- at 10 mM), HAB1-CsPYL1-NR (NR -*Nicotinamide Ribose*- at 5mM), HAB1-CsPYL1-NR (NR -*Nicotinamide Ribose*- at 500 µM), HAB1-CsPYL1-NR (NR -*Nicotinamide Ribose*- at 100 µM) and HAB1-CsPYL1-NR (NR -*Nicotinamide Ribose*- at 10 µM).
Thus, the different samples were prepared adjusting to a final reaction volume of 100 µL containing, in addition to the mentioned ratios of HAB1 phosphatase, CsPYL1 receptor and NR; DTT (dithiothreitol) and $MnCl_2$ at 1 mM concentration and pNPP at 25 mM.

For each sample, 4 replicates were performed. These replicates were arranged in a 96-well plate and their absorbances were measured at 405 nm at 0 min and 15 min. The absorbances were measured on the Bio-Rad ™ 3550 Microplate Reader.

In addition, the same assay was performed using CsPYL1 5M and CsPYL1 L195C receptors instead of CsPYL1 (CsPYL1 WT).

The percentage phosphatase activity of each sample was calculated in the same way as in the previous assay (3.3.1 HAB1 phosphatase activity assay). Then, once the percentage activity of each sample was obtained, GraphPad Prism 9.0 software was used to calculate and obtain the IC_{50} for the three cases (HAB1:CsPYL1 WT:NR complex, HAB1:CsPYL1 5M:NR complex and HAB1:CsPYL1 L195C:NR complex). For this purpose, a normalisation of the data was performed, including the transformation of NR concentrations to logarithmic scale.

4. RESULTS

4.1 The analysis of the ligand-receptor interactions

The success of a campaign of structure-based screening of bioactive compounds largely depends on the analysis and the precise definition of the structural determinants of the ligand binding to the target molecule. Thus, we analysed the interaction pattern observed in the experimentally determined ligand-receptor structures to implement this information in the subsequent docking protocol. This was focused mainly on the analysis of the structure of *Latch* and *Gate* loops on the ligand-receptor complexes; and also, on the polar interactions that those ligands established directly with the receptor or indirectly through water molecules.

To study the interactions between ABA and the receptor, the X-Ray Diffraction-structures of the ternary complex CsPYL1-ABA-HAB1 (CsPYL1 being an ABA receptor from *Citrus sinensis,* and HAB1 a PP2C-type phosphatase) and the CsPYL1 dimeric receptor were compared. Those correspond to 5MN0 and 5MMQ codes of the Protein Data Bank (PDB).

For the study of the interactions between the Nicotinic Acid and the receptor, the structures from PDB 7Z1S and 5MOA , also obtained by X-Ray Diffraction, were

compared. In this case, the 7Z1S structure corresponded to the SlPYL1-Nicotinic Acid complex (SlPYL1 being an ABA receptor of *Solanum lycopersicum*); and the 5MOA structure corresponded to the SlPYL1 receptor.

In addition, to better understand the behaviour of ABA receptors upon ligand binding, the PDB structures 8AY3 and 4LG5, both also obtained by X-Ray Diffraction, were also analysed. The 8AY3 structure corresponded to the ternary complex CsPYL1-iSB09-HAB1 and the 4LG5 structure to the ternary complex PYL2-Quinabactin-HAB1 (PYL2 being an ABA receptor of *Arabidopsis thaliana*). Both molecules, isB09 and Quinabactin, have previously been reported as ABA agonists [(23), (24)].

4.1.1 ABA's binding site interactions

The preliminary analysis of the structures of the dimeric CsPYL1 receptor and the CsPYL1-ABA-HAB1 ternary complex reveals that CsPYL1 requires dissociation to interact with HAB1 as the receptor shares dimerization and HAB1 interfaces (***Figure 2***).

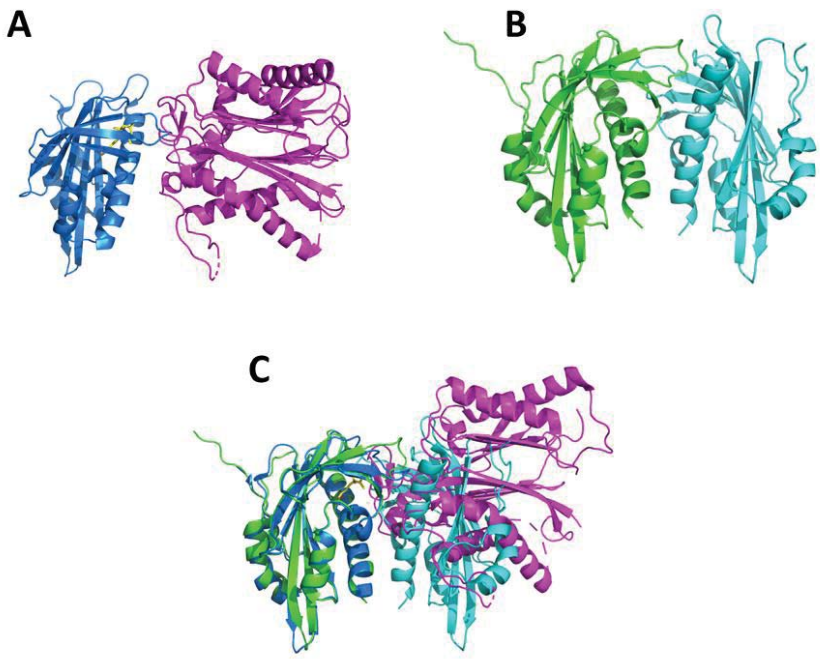

Figure 2. Requirement for dissociation of the dimeric form of the CsPYL1 receptor to allow entry of ABA to the binding site, and binding of HAB1 phosphatase. (A) CsPYL1-ABA-HAB1 ternary complex. **(B)** Dimeric form of CsPYL1 receptor. **(C)** CsPYL1-ABA-HAB1 ternary complex overlapping to the dimeric form of CsPYL1

receptor.

Regarding the structure of the *Latch* and *Gate* loops in the presence and absence of ABA at the CsPYL1 binding site, it was observed that, in the open form of the receptor (i.e. without ABA), the hydrophobic residues of the amino acids forming gate loop are facing outwards, whereas, in the closed form of the receptor (i.e. after the entry of ABA into the binding site and the binding of the HAB1 phosphatase to the complex), the hydrophobic residues are folded inwards, making them inaccessible to the water molecules in the environment. When ABA is at the binding site of the CsPYL1 receptor and HAB1 phosphatase binds to the complex, both *Latch* and *Gate* loops are closed, resulting in receptor folding (***Figure 3).***

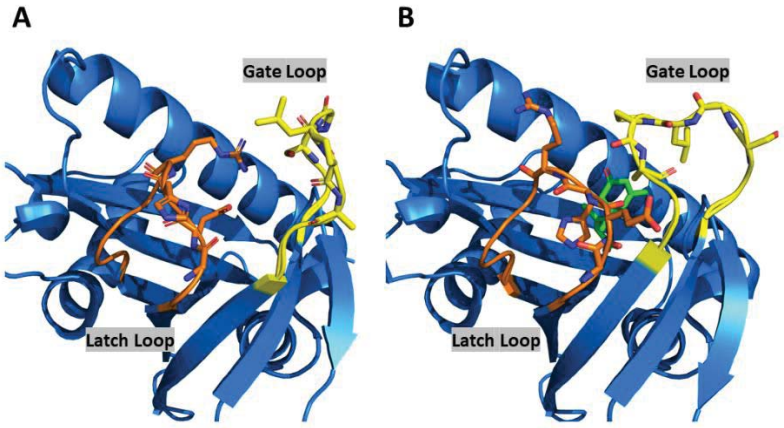

Figure 3. Behaviour of Latch and Gate loops. (A) Open form, CsPYL1 receptor without ABA bound. **(B)** Closed form, ABA hosted in the binding site of the CsPYL1 receptor and HAB1 bound to the complex.

Finally, with regard to the polar interactions between ABA and CsPYL1, two main areas of interaction were observed: through the carbonyl group and the carboxyl group of ABA. The carbonyl group of ABA interacts via hydrogen bond with a water molecule that also interacts with an Arginine residue located in the *Latch* loop of the CsPYL1 receptor (Arg-145), a Proline residue located in the *Gate* loop of the CsPYL1 receptor (Pro-117) and a Tryptophan residue belonging to the HAB1 phosphatase (Trp-385). On the other hand, the carboxyl group of ABA interacts with the receptor directly via hydrogen bond with a Lysine (Lys-88) residue and indirectly via hydrogen bonds with 3 water molecules that, at the same time, interact with other receptor residues (His-89, Tyr-149, Ser-151, Glu-170 and Asn-196) (***Figure 4***).

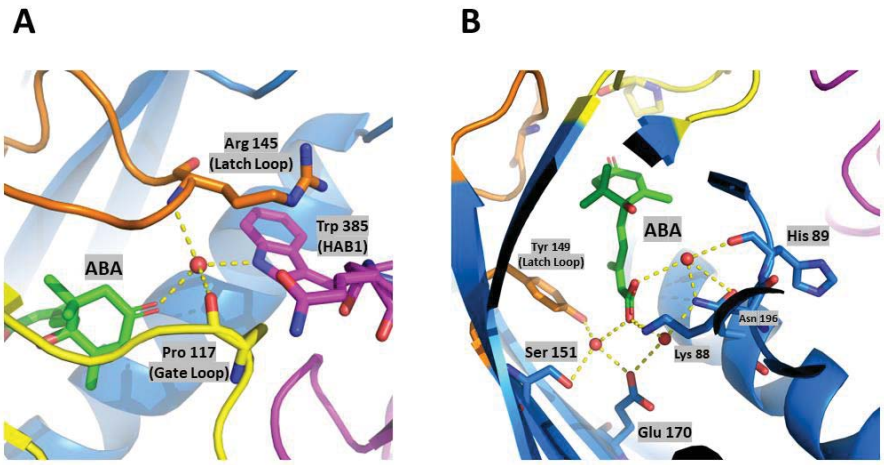

Figure 4. ABA-CsPYL1 polar interactions. (A) Through the carbonyl group of ABA. **(B)** Through the carboxyl group of ABA.

4.1.2 Nicotinic Acid's binding site interactions

The structure of the *Latch* and *Gate* loops in the presence and absence of Nicotinic Acid at the SlPYL1 binding site is similar to that observed for the complex with ABA. Thus, in the open form of the receptor (i.e. without Nicotinic Acid), the hydrophobic residues of the amino acids were facing outwards, whereas in the closed form of the receptor (i.e. after the entry of Nicotinic Acid into the binding site), the hydrophobic residues were folded inwards, making them inaccessible to the water molecules in the environment. When Nicotinic Acid is at the binding site of the SlPYL1 receptor, both *Latch* and *Gate* loops are closed, resulting in receptor folding (***Figure 5***).

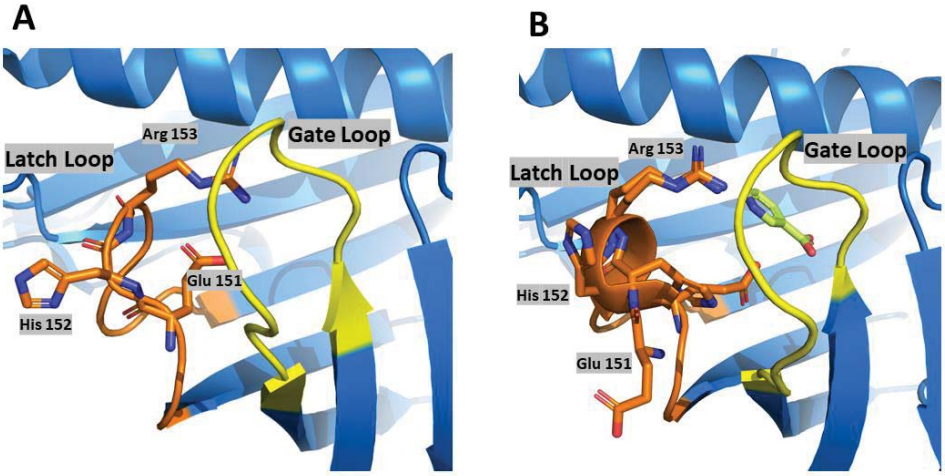

Figure 5. Behaviour of Latch and Gate loops. (A) Open form, SlPYL1 receptor without bound Nicotinic Acid. **(B)** Closed form, Nicotinic Acid lodged in the SlPYL1 receptor binding site.

Regarding the polar interactions between Nicotinic Acid and SlPYL1, one main site of interaction was observed: via the carboxyl group of Nicotinic Acid. The carboxyl group of Nicotinic Acid interacts with the receptor directly via an hydrogen bond with a Lysine residue (Lys-96) and indirectly via hydrogen bonds with 4 water molecules that interact with other residues of the receptor (Glu-131, Arg-116, Asn-204, Glu-178, Ser-159 and Tyr-157) (***Figure 6***).

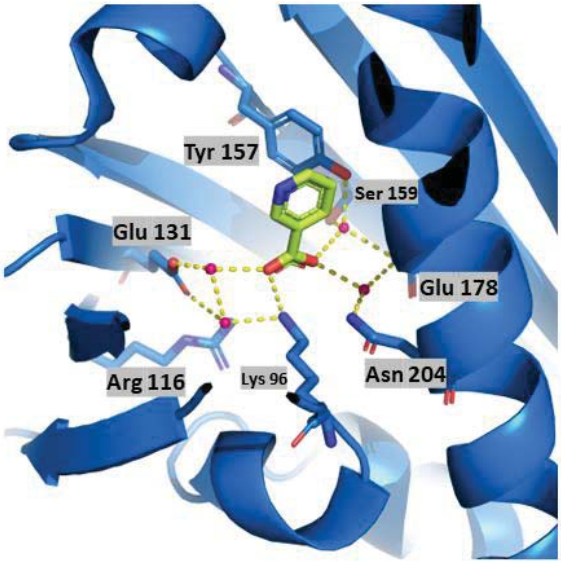

Figure 6. Nicotinic Acid-SlPYL1 polar interactions through the carboxyl group of Nicotinic Acid.

4.1.3 iSB09 and Quinabactin's binding site interactions

Additionally, the comparison of the interactions, both polar and hydrophobic, established by the known agonist molecules iSB09 and Quinabactin [23], [24] were analysed and compared with those established by ABA (***Table 1***):

MOLECULE	POLAR INTERACTIONS	HYDROPHOBIC INTERACTIONS	PRINCIPAL DIFFERENCES
ABA 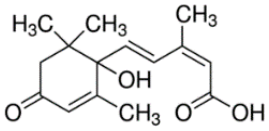	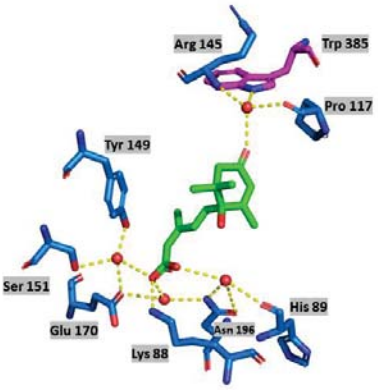	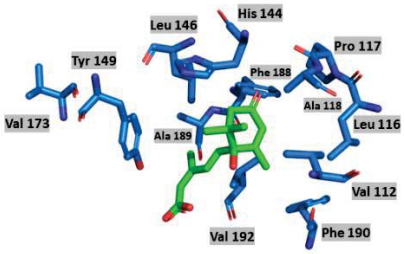	ABA interacts directly with one Lysine residue (Lys-88) and indirectly with other residues (His-89, Tyr-149, Ser-151, Glu-170 and Asn-196) via 3 water molecules.
Quinabactin 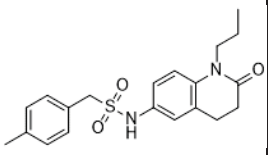	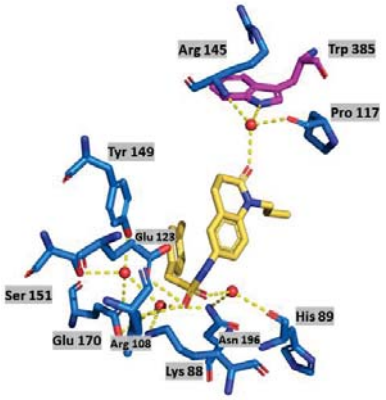	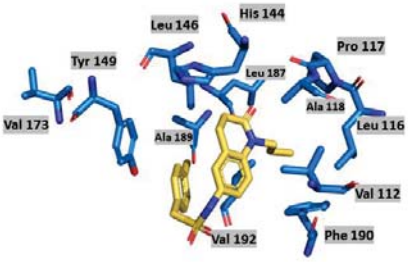	Quinabactin interacts directly with an Arginine residue (Arg-108) and a Glutamic Acid residue (Glu-123) and indirectly with other residues (His-89, Asn-196, Glu-170, Lys-88, Tyr-149 and Ser-151) via 3 water molecules.
iSB09			iSB09 interacts directly with a Lysine residue (Lys-88), an Arginine residue (Arg-108) and a Glutamic Acid

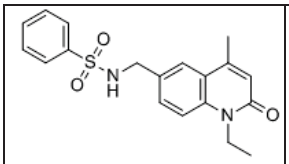	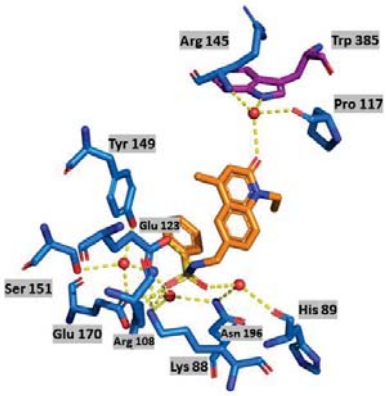	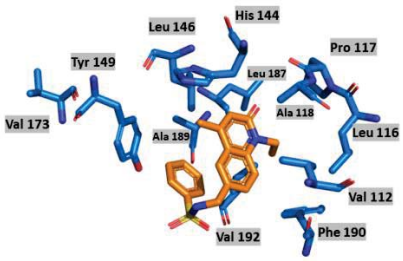	residue (Glu-123) and indirectly with other residues (His-89, Glu-170, Asn-196, Lys-88, Tyr-149 and Ser-151) via 3 water molecules.

Table 1. Polar and hydrophobic interactions of the ligands ABA, Quinabactin and iSB09.

4.2 Docking protocol, predictions and selected molecules

The docking protocol was firstly designed around the interactions between nicotinic acid and the ABA receptor because of the recent discovery of Nicotinic Acid as an ABA antagonist [16]. Therefore, it was decided to take this molecule as a starting point to find environmentally friendly agrochemical compounds capable of, exogenously, controlling the ABA-dependent response and thus, the response to drought stress.

The protocol created focused on the construction of a pharmacophore -*defined as a set of steric and electronic features necessary to ensure optimal supramolecular interactions with a specific biological target and to trigger (or block) its biological response* [25]- containing the following 4 regions (***Figure 7***): an aromatic ring centre in the benzene ring of the ligand, two hydrogen bond acceptor regions at the carboxyl end and an hydrophobic region located in the vicinity of the His-144 residue in the *Latch* loop of the receptor. The orientation of this residue towards the inside of the pocket is fundamental to allow the closure of the *Latch* loop of the receptor; thus, it is important to define the latter hydrophobic region. For a more precise definition of the pharmacophore, this hydrophobic region was matched to the original location of the methyl group of ABA, simulating the actual hydrophobic interaction that occurs between ABA and the receptor. (The exact coordinates of these regions and their values in the protocol can be found in **Table 4**, ***Annex***).

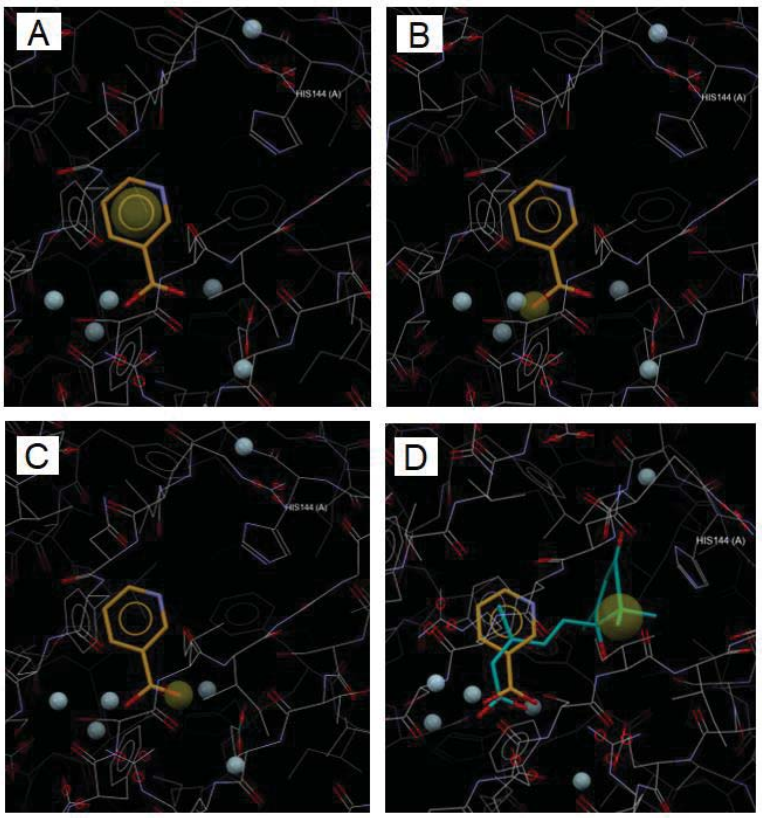

Figure 7. Defined regions in the pharmacophore. (A) Aromatic ring centre located in the benzene ring. **(B, C)** Hydrogen bond acceptors located at the carboxyl end **(D)** Hydrophobic region located in the vicinity of the His-144 residue of the *Latch* loop.

After analysing the scores obtained in the docking studies with the different ligands of the self-made database, 4 candidate molecules were detected: 2 potential agonists (Nicotinamide Ribose -*NR*- and Ribosylnicotinate -*R*-) and 2 potential antagonists (Nicotinamide mononuclotide -*Nmn*- and Nicotinate Beta-D-Ribonucleotide -*β-R*-) of Nicotinic Acid. The potential agonist ligands not only had high scores, but also the generated poses or predicted structures, were physico-chemically correct and promising (***Table 2***). On the other hand, the potential antagonist ligands had lower scores and also, poses that suggested that it would be impossible for HAB1 phosphatase to bind to the complex due to the space that the phosphate group of these ligands occupied in the binding site.

LIGAND ID & STRUCTURE	TYPE	DOCKING PREDICTION	SCORE
Nicotinamide Ribose (ZINC4096036) 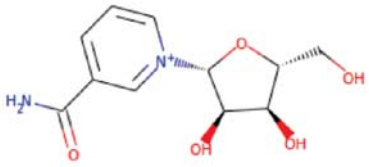	Agonist	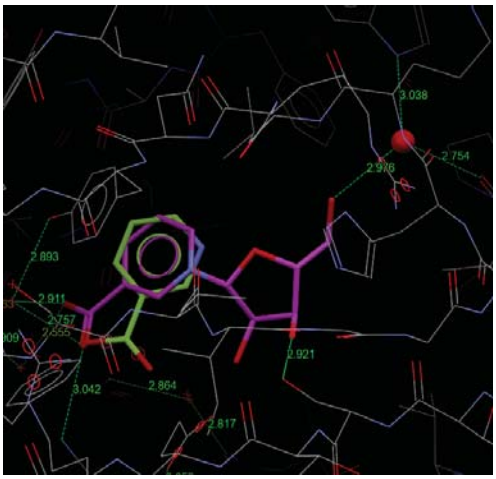	79.3/100
Ribosylnicotinate (ZINC4096931) 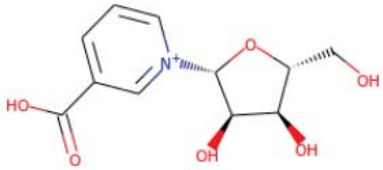	Agonist	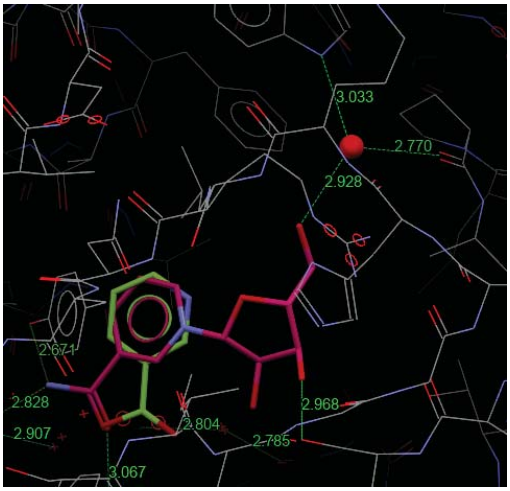	86.1/100
Nmn (ZINC4228273) 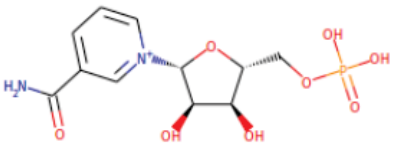	Antagonist	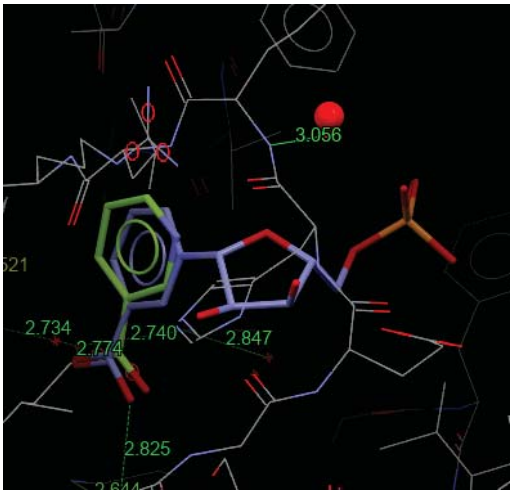	73.7/100

Nicotinate Beta-D-Ribonucleotide (ZINC4095572) 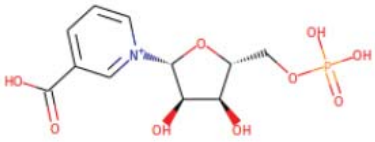	Antagonist	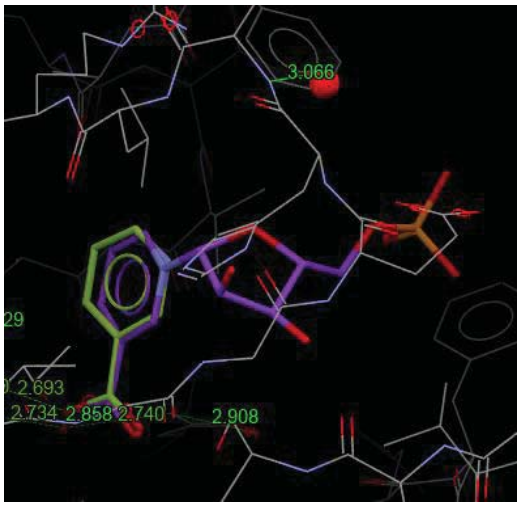	74.5/100

Table 2. The 4 candidate environmentally friendly agrochemical compounds. In the table are shown the ligands' ID and structures, their type, the docking prediction compared to the control ligand (Nicotinic Acid) and the docking score.

4.3. Expression and purification of proteins

To perform the experimental validation of the hits obtained from the docking studies, the CsPYL1 receptor was expressed and purified.

After the expression and purification processes carried out, the overall yield of CsPYL1 production by E.coli was 11.8 mg per litre of culture.

As mentioned above, to check the purity of the protein and the quality of the purification process, a 12% acrylamide SDS-PAGE gel electrophoresis was performed. Thus, the following samples were loaded in the gel and analysed (***Figure 8***):

- **Mw**: molecular weight standard. The 25 kDa band is highlighted and serves as a guide
  as the molecular weight of CsPYL1 is 24.06 kDa.
- **PF**: precipitate fraction. I.e. a sample of the pellet obtained after expression of CsPYL1. The sample contains impurities.
- **FT**: flow through collected after passing the soluble fraction through the Nickel (N^{2+}) column. Sample contains impurities and some CsPYL1.
- **W1**: wash fraction collected after passing 10 column volumes of base buffer.

Contaminating protein and CsPYL1 are observed.

- **W2**: wash fraction collected after passing 10 column volumes of base buffer supplemented with 40 mM imidazole. Contaminating protein and CsPYL1 are observed.
- **PD**: post-dialysis. Shows the content found inside the membrane after dialysis. One of the bands corresponds to CsPYL1, there is also a slightly higher molecular weight band corresponding to TEV protease (27 kDa approximately) and impurities can also be seen.
- **Imdz**: sample collected from the Nickel column after washing with imidazole after eluting the protein sample. As can be seen, only impurities come out, indicating that the chromatography was performed correctly.
- **Pre-SEC**: samples pooled before undergoing SEC chromatography. CsPYL1 is shown.
- **Post-SEC**: sample eluted after SEC chromatography. Pure CsPYL1 protein is shown.

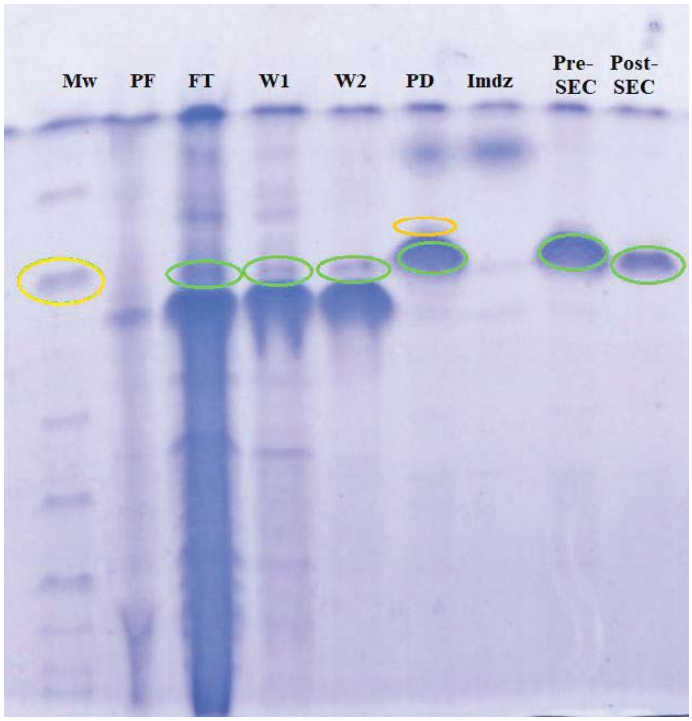

Figure 8. SDS-PAGE gel electrophoresis. Reference band of 25 kDa surrounded in yellow. Surrounded in green CsPYL1 (24.06 kDa). Surrounded in orange TEV protease (approximately 27 kDa).

Finally, following size-exclusion chromatography, a profile of the CsPYL1 protein was generated by plotting the absorbances of the samples obtained from SEC against the flow rate, resulting in a chromatogram.

The profile obtained shows a single asymmetric main peak indicating the protein fractions of CsPYL1 corresponding to this peak were homogeneous enough to perform subsequent biochemical assays (***Figure 9***).

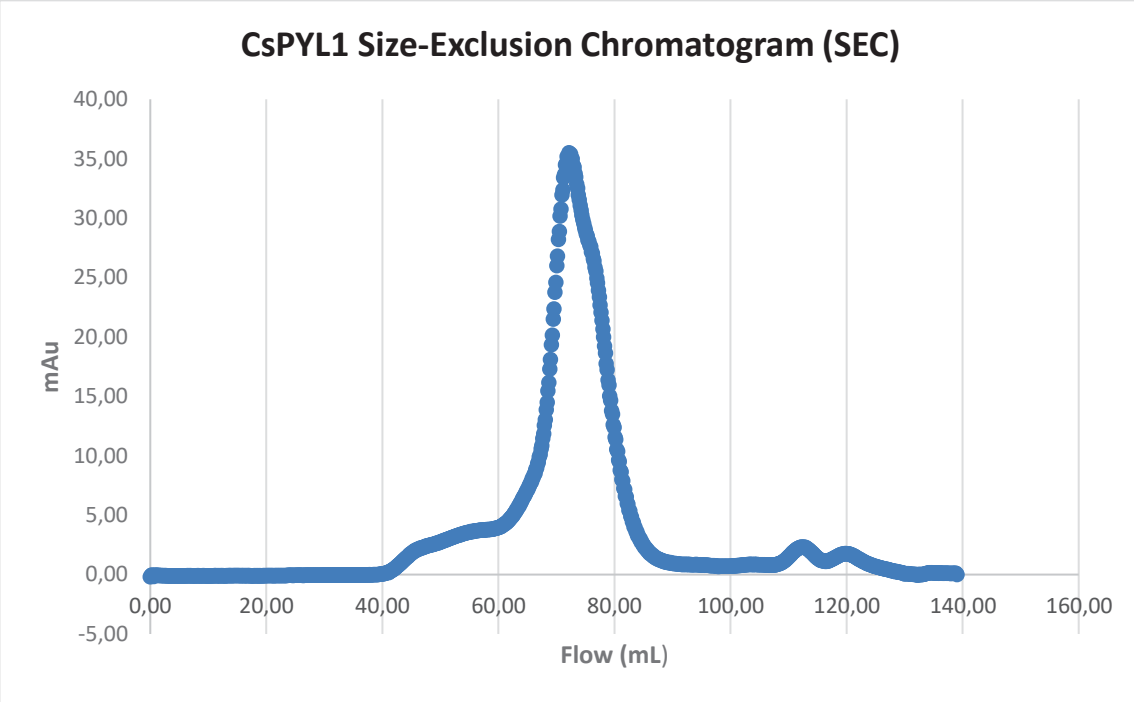

Figure 9. CsPYL1 Size-Exclusion Chromatogram. The main peak refers to the CsPYL1 dimer. The small peaks at the end indicate low molecular weight impurities.

4.4 Affinity studies

4.4.1 HAB1 phosphatase activity assay

To evaluate the binding capacity between the CsPYL1 receptor and the different hits obtained in the docking studies, phosphatase activity assays were performed.

This assay determines the percentage of HAB1 phosphatase activity. As initially mentioned, the formation of the HAB1-CsPYL1-ABA ternary complex involves the inhibition of HAB1 phosphatase. The binding of the CsPYL1 receptor slightly inhibits the phosphatase and binding of ABA completely inhibits the phosphatase, forming the

ternary complex. Thus, by assaying with the different candidate compounds, we can determine, through the resulting phosphatase activity, the extent to which these compounds bind to the receptor and phosphatase, forming a ternary complex. In other words, this phosphatase activity assay is an indirect measure of the affinity of the ligands for the complex.

The key element for this phosphatase activity assay is pNPP (p-nitrophenyl phosphate). This substrate is capable of being hydrolysed by the phosphatase HAB1, giving rise to a phenolic yellow compound (***Figure 10***) that absorbs at a wavelength of 405 nm. In this way, the course of this reaction can be measured, and therefore, the percentage of phosphatase activity can be obtained.

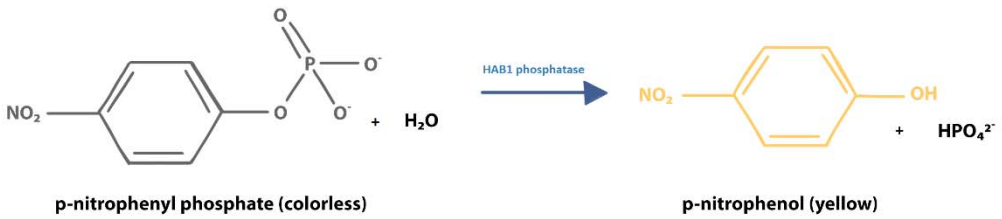

Figure 10. PNPP reaction. The action of HAB1 phosphatase on pNPP results in a yellow phenolic compound.

Our data showed that out of the four ligands assayed NR display significant inhibition of the HAB1 activity (***Figure 11***). It is worth to note, that we additionally observed some ABA independent inhibition by CsPYL1.

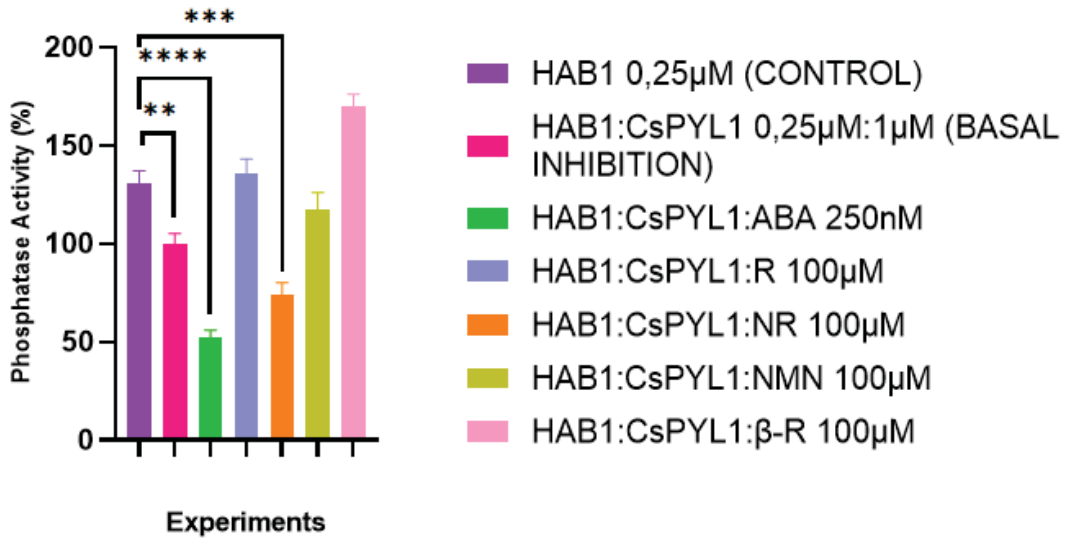

Figure 11. Phosphatase activity assay results. From left to right: HAB1 control at 0.25 µM; HAB1-CsPYL1 at 0.25 µM : 1 µM ratio (1: 4); HAB1-CsPYL1-ABA (ABA at 250 nM), HAB1-CsPYL1-R (R -Ribosylnicotinate- at 100 µM), HAB1-CsPYL1-NR (NR -Nicotinamide Ribose- at 100 µM), HAB1-CsPYL1-Nmn (Nmn -Nicotinamide mononucleotide- at 100 µM) and HAB1-CsPYL1-β-R (β-R -Nicotinate Beta-D-Ribonucleotide- at 100 µM). Note: in ligand-bound samples, HAB1 and CsPYL1 are always in a 1:4 ratio (0.25 µM HAB1 : 1 µM CsPYL1). Values represent the mean ± SD of the four replicates performed for each sample. Asterisks indicate statistical significance (* p-value < 0.05, ** p-value < 0.01 and *** p-value < 0.001) in Student's t-test compared to the corresponding control (HAB1).

4.4.2 IC_{50} curves

The IC_{50} value is defined as the concentration of ligand capable of inhibiting the HAB1 phosphatase activity by 50%. Therefore, the higher the IC_{50} value, the worse the affinity of the ligand for the ternary complex. To determine this value we monitored phosphatase activity at increasing ligand concentration and adjust a function relating activity versus the logarithm of this concentration. Following the results obtained in the HAB1 phosphatase activity assay, the IC_{50} of the agonist compound NR, which was found to be able to form a ternary complex together with HAB1 and CsPYL1, was calculated.

We perform IC_{50} calculations for ligand NR using CsPYL1 and two mutant proteins CsPYL1 L195C and CsPYL1 5m [23]. These mutant proteins were designed to represent the different properties of the isoforms of PYL receptors while harbouring a common tertiary structure. While CsPYL1 L195C is monomeric (A. Albert communication) the CsPYL1 5m is dimeric but present the ABA binding pocket of monomeric receptors [23].

The results obtained were an IC_{50} of 0.54 ± 0.05 mM for the WT, an IC_{50} 0.52 ± 0.06 mM for the L195C mutant and an IC_{50} of 1.28 ± 0.06 mM for the 5M mutant (***Figure 12***).

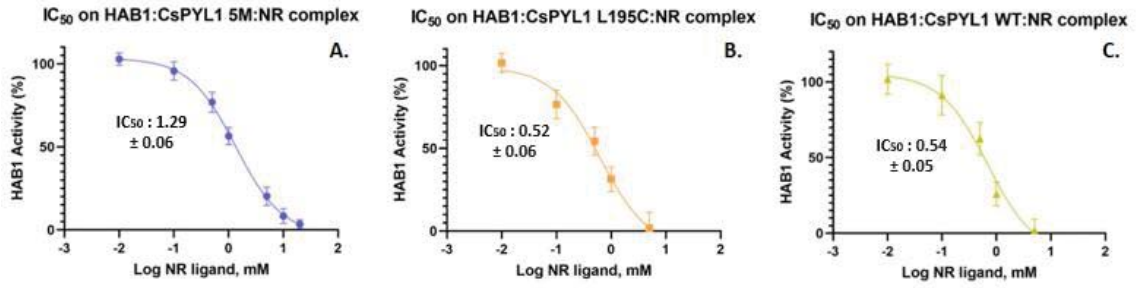

Figure 12. IC_{50} curves of compound NR forming the ternary complex with HAB1 and different CsPYL1 receptors. (A.) CsPYL1 5M receptor. The IC_{50} value is 1.28 ± 0.06 mM. **(B.) CsPYL1 L195C receptor.** IC_{50} value is 0.52 ± 0.06 mM **(C.) CsPYL1 WT Receptor**. IC_{50} value is 0.54 ± 0.05 mM.

5. DISCUSSION

The comparative analysis of the structures of the apo forms of CsPYL1 and SlPYL1, and their complexes with HAB1 and ABA, Nicotinic Acid and other known agonist molecules corroborated the previously reported structural basis for ligand recognition and subsequent inhibition of HAB1 [14]. They involve receptor dimer dissociation, a conformation rearrangement of *Gate* and *Latch* loops, to accommodate the ligand, and the interaction with the HAB1 active site. The role of the HAB1 phosphatase as a co-receptor was also corroborated, as it interacts indirectly, in all cases, with the ligand through a water molecule, thus allowing the formation of the ternary complex.

The results of docking studies performed on the designed protocols suggested 4

compounds as possible candidates for environmentally friendly agrochemical compounds: 2 possible agonists (NR -*Nicotinamide Ribose*- and R -*Ribosylnicotinate*-) and 2 possible antagonists (Nmn -*Nicotinamide mononucleotide*- and β-R -*Nicotinate Beta-D-Ribonucleotide*-) of Nicotinic Acid. Both 4 obtained high scores and physico-chemically correct and promising poses.

Interestingly, NR ligand showed significant inhibition of phosphatase activity (***Figure 11***). Therefore, indicating that the docking protocol is accurate enough as to identify bioactive compounds. Conversely, neither the R ligand nor the NMN ligand, nor the β-R ligand showed significant inhibition of phosphatase activity (***Figure 11***). The results for the NMN and β-R ligands are expected as our predictions suggested an ABA-antagonist activity for both. This antagonistic activity resides in the presence of a phosphate group which is oriented towards the outside of the binding cavity as it is structurally too large to converge in the pocket (***Table 2***), thus hindering the interaction with the phosphatase.

The IC_{50} determination for NR ligand showed that the IC_{50} value using the wild-type receptor was 0.54 ± 0.05 mM, which is larger than those reported for other known agonist molecules which are in sub μM range [23]. The IC_{50} value observed using the CsPYL1 L195C receptor was almost identical to that determined for the WT proteins (0.52 ± 0.06 mM). This is unexpected as this mutant receptor is monomeric; therefore, this indicates that there is no energetic penalty associated with the dissociation of the dimeric receptors for the formation of the ternary complex with the phosphatase. The highest IC_{50} value was for the complex containing the CsPYL1 5M receptor (1.28 ± 0.06 mM). This result indicates that the mutations (F137I and V112L) at the binding site might hinder NR interaction with the receptor.

As known, Nicotinic Acid (used as a control molecule to design the docking protocol) is a precursor of NAD (nicotinamide adenine dinucleotide), a compound widely present in plant cells [17]. In fact, compounds NR and Nmn are also precursors of NAD as can be seen in the following image (***Figure 13***). Therefore, NR might constitute an environmentally friendly agrochemical candidate compound to regulate the control of the ABA-dependent response of the pathway, because although it is required in the mM range, it comes from a precursor present in the cell whose concentration is around 0.2 and 0.5 mM [26]. Hence, it is expected that the exogenous addition of this compound at that

concentration would not result in negative effects for the plant. In order to corroborate this, future in vitro assays on the rest of the receptors of the family and in vivo assays in plants should be carried out.

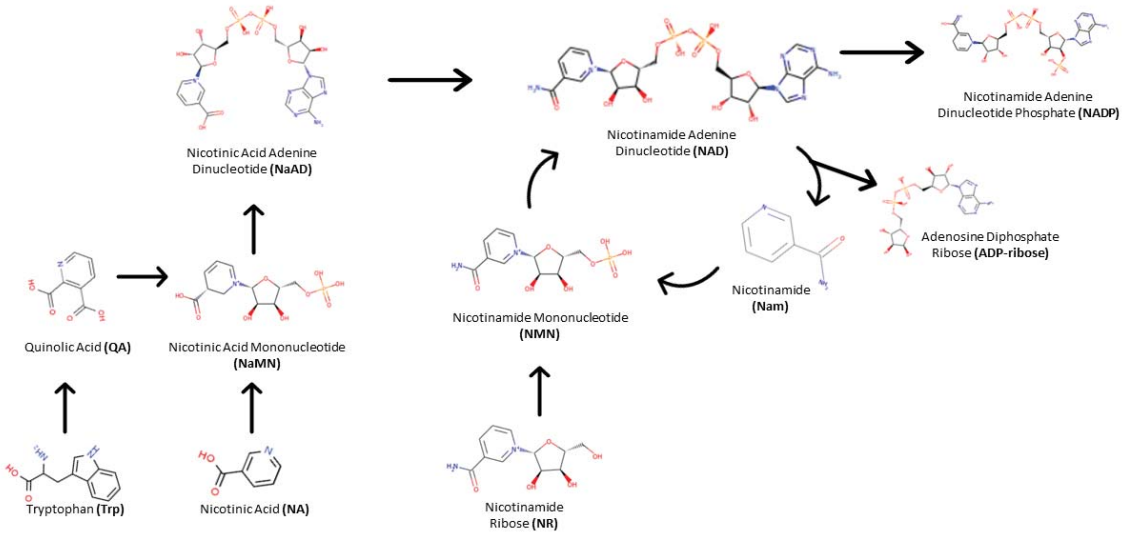

Figure 13. NAD biosynthesic pathway.

Finally, it should be emphasised that the use of bioinformatics was fundamental to optimise the implementation of this research project, as the creation of a database of natural compounds from an *in silico* screening using tools such as Arthor, Coot and Mercury; and the prediction of possible candidate compounds through the creation of protocols and the performance of studies in GOLD meant a significant saving in time and money resources. Moreover, the use of PyMOL for interaction studies allowed us to easily and quickly obtain a high level of precision and detail of ligand-protein behaviour. The curated database and the docking protocol designed along this work could be employed for the discovery of other compounds based on different target receptor structures in future work.

6. CONCLUSIONS

1. The comparative analysis of the structures of the apo forms of CsPYL1 and SlPYL1, and their complexes with HAB1 and ABA, Nicotinic Acid and other known agonist molecules corroborate the previously reported structural basis for ligand recognition and subsequent inhibition of HAB1.

2. A docking protocol and a database have been created to allow the identification of potential ABA agonists and antagonists, saving significant resources in terms of money and time.

3. Experimental analysis of the docking hits unravels that NR -*Nicotinamide Riboside*- is a bioactive molecule.

4. The use of bioinformatics and computational tools in this research project is suitable for the identification of potential ABA agonists and antagonists.

5. BIBLIOGRAPHY

1. Nelson, G. C., Rosegrant, M. W., Koo, J., Robertson, R., Sulser, T., Zhu, T., Ringler, C., Msangi, S., Palazzo, A., Batka, M., Magalhaes, M., Valmonte-Santos, R., Ewing, M., Lee D. (2009). *Cambio climático el impacto en la agricultura y los costos de adaptación*. IFPRI.
2. Valladares, F., Vilagrosa, A., Peñuelas, J., Ogaya, R., Camarero, J. J., Corucera, L., Sisó, S., Gil-Pelegrín, E. (2004). *Ecología del bosque mediterráneo en un mundo cambiante*. Capítulo 6 – Estrés hídrico: ecofisiología y escalas de la sequía. Pages 163-190. Ministerio de Medio Ambiente.
3. Lambers H., Chapin F.S., Pons T.L. (1998). *Plant Physiological Ecology*. Springer-Verlag.
4. Nilson, S. E., & Assmann, S. M. (2007). The control of transpiration. insights from Arabidopsis. *Plant Physiology*, *143*(1), 19–27. DOI: 10.1104/pp.106.093161
5. Beadle, C. L. (1987). CHAPTER 5 - WATER RELATIONS. *Techniques in bioproductivity and photosynthesis (Second Edition).* Pages 50-61. Pergamon International Library of Science, Technology, Engineering and Social Studies.
6. Busk, P.K., Pagés. M. (1998). Regulation of abscisic acid-induced transciption. *Plant Mol. Biol. 37*, 425-435. DOI: 10.1023/a:1006058700720
7. Leung, J. y J. Giraudat. (1998). Abscisic acid signal transduction. *Ann. Rev. plant Physiol. Plant Mol. Biol. 49*, 199-222. DOI: 10.1146/annurev.arplant.49.1.199
8. Bray, E.A. (1991). Regulation of gene expression by endogenous ABA during drought stress. *Bios Scientific Publisher*, 81-96.
9. Zhang S.Q. y W.H Outlaw. (2001). Abscisic acid introduced into the transpiration stream accumulates in the guard cell apoplast and causes stomatal closure. *Plant Cell Environ. 24*, 1045-1054.
10. Roelfsema, M.R.G. y R. Hedrich. (2002). Studying guard cell in the intact plant: modulation of stomatal movement by apoplastic factors. *New Phytol. 153*, 425-431. DOI: 10.1046/j.0028-646X.2001
11. Rodriguez, P.L., Lozano-Juste, J., & Albert, A. (2019). PYR/PYL/RCAR ABA receptors. *Advances in Botanical Research*. DOI:10.1016/BS.ABR.2019.05.003
12. Santiago, J., Dupeux F., Round, A., Antoni, R., Park, S.Y., Jamin, M., Cutler S. R., Rodriguez, P. L., Marquez, J. A. (2009). The abscisic acid receptor PYR1 in complex with abscisic acid. *Nature 462*, 665-668. DOI: 10.1038/nature08591
13. Dupeux, F., Santiago, J., Betz, K., Twycross, J., Park, S. Y., Rodriguez, L., Gonzalez-Guzman, M., Jensen, M. R, Krasnogor, N., Blackledge, M. Holdsworth, M., Cutler, S. R., Rodriguez, P. L., Marquez J. A. (2011). A thermodynamic switch modulates abscisic acid receptor sensitivity. *EMBO J 30*, 4171-4184. DOI: 10.15252/embj.2022110799
14. Moreno-Alvero, M., Yunta, C., Gonzalez-Guzman, M., Lozano-Juste, J., Benavente, J. L., Arbona, V., Menendez, M. Martinez-Ripoll, M., Infantes, L, Gomez-Cadenas, A., Rodriguez, P. L., Albert, A. Structure of Ligand-Bound Intermediates of Crop ABA Receptors Highlights PP2C as Necessary ABA Co-receptor. (2017). *Mol Plant 10*, 1250-1253. DOI:10.1016/j.molp.2017.07.004
15. Hewage, K. A. H., Yang, J. F., Wang, D., Hao, G. F., Yang, G. F., and Zhu, J. K. (2020). Chemical Manipulation of Abscisic Acid Signaling: a New Approach to Abiotic and Biotic Stress Management in Agriculture. *Adv. Sci. 7*:2001265. DOI: 10.1002/advs.202001265

16. Infantes, L., Rivera-Moreno, M., Daniel-Mozo, M., Benavente, J.L., Ocaña-Cuesta, J., Coego, A., Lozano-Juste, J., Rodriguez, P.L., Albert, A. (2022) Structure-Based Modulation of the Ligand Sensitivity of a Tomato Dimeric Abscisic Acid Receptor Through a Glu to Asp Mutation in the Latch Loop. *Front. Plant Sci. 13*:884029. DOI: 10.3389/fpls.2022.884029
17. Alferez, F. M., Gerberich, K. M., Li, J. L., Zhang, Y., Graham, J. H., and Mou, Z. (2018). Exogenous Nicotinamide Adenine Dinucleotide Induces Resistance to Citrus Canker in Citrus. Front. *Plant Sci. 9*:1472. DOI: 10.3389/fpls.2018.01472
18. DeLano, L. Schrödinger, Ed. (2002).
19. Irwin, J. J. et al. (2020). ZINC20 -a free ultralarge- scale chemical database for ligand discovery. *J. Chem. Inf. Model. 60*, 6065–6073.
20. Emsley, P., Cowtan, K. (2004). Coot: model-building tools for molecular graphics title. *Acta Crystallogr D Biol 986 Crystallogr 60*, 2126-2132.
21. Groom, C. R., Bruno, I. J., Lightfoot, M. P., Ward, S. C. (2016). The Cambridge Structural Database. *Acta Crystallogr 970 B Struct Sci Cryst Eng Mater 72*, 171-179.
22. Jones, G., Willett, P., Glen, R. C., Leach A. R., Taylor R. (1997). Development and validation of a genetic algorithm 960 for flexible docking. *J Mol Biol 267*, 727-748.
23. Lozano-Juste, J., Infantes, L., García-Maquilon, I., Ruiz-Partida, R., Merilo, E., Benavente, J.L., Velazquez-Campoy, A., Coego, A., Bono, M., Forment, J., Pampín, B., Destinto, P., Monteiro, A., Rodriguez, R., Cruces, J., Rodriguez, P.L., Albert, A. (2023). Structure-guided engineering of a receptor-agonist pair for inducible. *Sci. Adv. 9*, 10. DOI:10.1126/sciadv.ade9948
24. Cao, M., Liu, X., Zhang, Y., Xue, X., Zhou, X.E., Melcher, K., Gao, P., Wang, F., Zeng, L., Zhao, Y., Zhao,Y., Deng, P., Zhong, D., Zhu, J.K., Xu, H.E., Xu, Y. (2013). An ABA-mimicking ligand that reduces water loss and promotes drought resistance in plants. *Cell Res 23*, 1043-1054. DOI: 10.1038/cr.2013.95
25. Camillle G., Wermuth et al. (1988). Glossary of terms used in medicinal chemistry (IUPAC). *Pure Applied Chemistry 70*, 1129-1143.
26. Cantó, C., Menzies, K., Auwerx, J. NAD^+ metabolism and the control of energy homeostasis - a balancing act between mitochondria and the nucleus. *Cell Metabolism 22*, 31-53. DOI: 10.1016/j.cmet.2015.05.023

ANNEX

W1	HETATM	3835	O	HOH W	1	7.521	6.150	27.942	1.00 45.14	O
W2	HETATM	3834	O	HOH W	2	-1.425	8.783	34.065	1.00 47.67	O
W3	HETATM	3828	O	HOH W	3	-0.572	8.414	38.936	1.00 54.80	O
W4	HETATM	3820	O	HOH W	4	2.023	5.349	39.823	1.00 52.76	O
W5	HETATM	3881	O	HOH W	5	0.791	6.109	37.912	1.00 55.07	O
W6	HETATM	3842	O	HOH W	6	-3.744	4.034	34.654	1.00 54.75	O

Table 3. Water molecules coordinates included in the CsPYL1 mould file. Coordinates extracted from a MOL2 file.

The blue-labelled water is only found in iSB09, and the orange-labelled water is found neither in iSB09 nor Quinabactin (in fact, it was selected because it is located in the position occupied by one of the oxygens of the sulphonyl group of Quinabactin, which interacts directly with Arg-108 and Glu-123 residues). The rest of the waters are common to all experimental structures.

Region Type	Coordinates	Radius	Constraint Weight	Fitting point weight	Score contribution per atom found in region
Aromatic Ring Centre	3.1417 6.9365 35.316	1	30	3	-
H-Bond Acceptor	0.259 6.161 37.393	0.6	30	5	-
H-Bond Acceptor	-0.326 5.734 35.283	0.6	30	5	-
Hydrophobic Region	2.5200 4.5000 31.2100	1	-	-	5

Table 4. Exact coordinates of the pharmacophore regions and their corresponding values in the protocol.